JOURNAL OF GEOPHYSICAL RESEARCH, VOL. 112, D10S33, doi:10.1029/2006JD007581, 2007

Evaluation of the aerosol indirect effect using satellite, tracer transport model, and aircraft data from the International Consortium for Atmospheric Research on Transport and Transformation

L. Avey,[1] T. J. Garrett,[1] and A. Stohl[2]

Received 30 May 2006; revised 13 October 2006; accepted 6 December 2006; published 31 March 2007.

[1] The magnitudes of the ''indirect effects'' that anthropogenic aerosols have on clouds and climate remain uncertain. Past space-based characterizations have compared satellite retrievals of cloud properties with satellite- or model-derived aerosol quantities. The two fields have been taken from air masses displaced from each other either horizontally or vertically. Thus, almost by definition, the cloud retrievals have come from different meteorological regimes than the aerosol to which ostensibly they are related. Because cloud properties depend foremost on meteorology, the difference introduces undesired ambiguity in the comparisons. In this study, we compare Terra and Aqua Moderate Resolution Imaging Spectroradiometer (MODIS) cloud retrievals with high spatial and temporal resolution output from a tracer transport model (FLEXPART), enabling colocation of fields of pollution and clouds both vertically and horizontally. Anthropogenic carbon monoxide (CO) is used as a passive pollution tracer, because its concentrations are tied to mixing and pollutant source strength, and they are independent of atmospheric oxidation and removal processes on timescales of weeks to months. Cloud and pollution fields are compared along a downwind axis from the U.S. northeastern seaboard for the duration of the summer 2004 International Consortium for Atmospheric Research on Transport and Transformation (ICARTT) mission. Where the transport model indicates air as being polluted, cloud r_e is smaller and cloud optical depth is in some cases higher, at least close to primary source regions. However, within 4 ± 1 days advection time from the northeastern seaboard, cloud perturbations become negligible, probably because of wet-scavenging of CCN. No conclusive evidence was found for any perturbation to cloud liquid water path by pollution.

Citation: Avey, L., T. J. Garrett, and A. Stohl (2007), Evaluation of the aerosol indirect effect using satellite, tracer transport model, and aircraft data from the International Consortium for Atmospheric Research on Transport and Transformation, *J. Geophys. Res.*, *112*, D10S33, doi:10.1029/2006JD007581.

1. Introduction

[2] Known as the first indirect effect, it has been argued that the solar albedo of shallow layer clouds is higher under polluted conditions because increased concentrations of droplets correspond to smaller droplet radii and increased scattering cross-section densities [*Twomey*, 1977]. A second indirect effect is the hypothesized increase to cloud lifetime and cover [*Albrecht*, 1989] arising from a reduction to the precipitation water sink through slower cloud droplet collision-coalescence.

[3] Anthropogenic aerosol can be transported long distances from continental sources to remote oceanic locations, where they can result in higher cloud droplet number concentrations (N) and smaller cloud droplet effective radii (r_e) [*Garrett and Hobbs*, 1995; *Borys et al.*, 1998; *Lohmann and Lesins*, 2002]. Because marine low-level clouds are generally clean and lie over a dark ocean, their susceptibility to these ''indirect effects'' can be particularly large [*Platnick and Twomey*, 1994]. A contributing effect may be that, as pollution is transported, cloud oxidative processes add to particulate soluble mass, potentially creating more numerous and efficient cloud condensation nuclei (CCN) [*Hegg et al.*, 1980; *Hoppel et al.*, 1994; *Johnson et al.*, 2000; *Peäjä et al.*, 2005].

[4] Recently, satellite data has been applied to investigations of aerosol indirect effects on both regional and global scales [e.g., *Nakajima et al.*, 2001; *Bréon et al.*, 2002; *Sekiguchi et al.*, 2003; *Quaas et al.*, 2004; *Matheson et al.*,

[1]Meteorology Department, University of Utah, Salt Lake City, Utah, USA.
[2]Norwegian Institute for Air Research, Kjeller, Norway.

0148-0227/07/2006JD007581$09.00

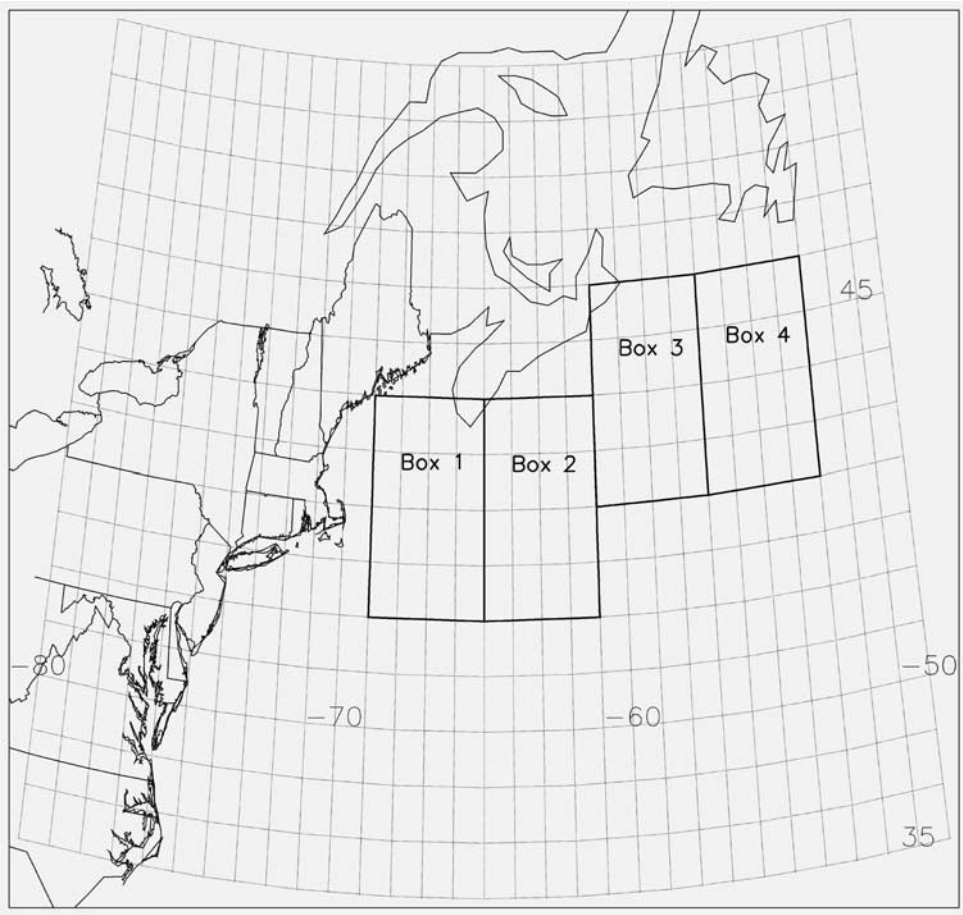

Figure 1. Four analysis boxes downwind of the U.S. northeastern seaboard used in this study. Each dashed line represents 1° of latitude and longitude.

2005; *Kaufman et al.*, 2005]. In particular, Moderate Resolution Imaging Spectroradiometer (MODIS) data from the Terra and Aqua satellites have been applied to constrain the indirect effect calculated in global circulation models [*Quaas and Boucher*, 2005; *Quaas et al.*, 2006] and to examine the effects of different aerosol types on MODIS derived low-level clouds over the Atlantic Ocean basin [*Kaufman et al.*, 2005]. A possible drawback with each of these studies is that passive satellite methods are unable to measure polluted and cloudy air in the same place. A common approach is to instead pair column aerosol retrievals with clouds in adjacent air masses. An assumption is then made that aerosol concentration fields are horizontally homogeneous between the cloudy and cloud-free regions [e.g., *Quaas et al.*, 2006].

[5] While this approach may be adequate for studies of convective clouds, which entrain and detrain CCN from adjacent clear regions over horizontal scales larger than the convective clouds themselves, it may be less suitable for studies of indirect effects on stratiform clouds. Because of their large and more uniform spatial coverage, adjacent masses of clear and cloudy air are more likely derived from different meteorological regimes, possibly even across frontal boundaries. Further, satellites are unable to locate aerosol pollutants in the vertical, and it is often assumed that the retrieved aerosol quantities are restricted to the boundary layer [e.g., *Matheson et al.*, 2005]. Over the northern Atlantic, however, pollution may be transported from North America to Europe in the upper troposphere within what is known as a "warm conveyor belt" [*Stohl*, 2001]. In this case, space-based observations of cloud and aerosol signatures could easily be derived from differing heights.

[6] An alternate strategy for employing satellite-based measurements is to use high temporal and spatial resolution output from a chemical transport model (CTM), and to colocate these pollutant fields with satellite retrievals of low-level cloud properties. This combination has been used previously to estimate indirect radiative forcing, either by pairing data ensembles [e.g., *Jones et al.*, 1994; *Chameides et al.*, 2002], or individual cells of CTM and satellite data [*Schwartz et al.*, 2002; *Kawamoto et al.*, 2006]. *Schwartz et al.* [2002], for example, used as a pollution tracer the sulfate column burden, which was calculated using primary SO_2 emissions based on mixing and prescribed modeled rates of oxidation and dry and wet deposition. These were then colocated with Advanced Very High Resolution Radiometer (AVHRR) cloud retrievals.

[7] There are two difficulties with this approach. First, for the same reasons described above, model column sulfate may be concentrated at a level different than the relevant cloud level. Second, a strict analysis of the sensitivity of cloud properties to pollution should exclude from its analysis any feedbacks associated with the sensitivities of pollution to clouds. For example, cloud processing may

make concentrations of CCN either lower (through precipitation) or higher (through aqueous phase oxidation), where the rate of processing is itself influenced by CCN effects on cloud properties. It is impossible to separate these complexities if the ''independent'' quantity used (e.g., column sulfate) is not, in fact, independent of the dependent cloud properties.

[8] To circumvent these issues, our approach here is to explore whether it is possible to objectively quantify aerosol indirect effects by horizontally and vertically colocating satellite retrievals of cloud properties with simulated distribution fields of a passive anthropogenic tracer. Here we use carbon monoxide (CO) as a model tracer. Although ostensibly any arbitrary tracer quantity could be used in a tracer model, using CO is physically realistic. This is because it has anthropogenic sources, it is insoluble in cloud water, and it oxidizes over weeks to months rather than hours to days. Thus, even in nature its concentrations are largely independent of all atmospheric processes besides mixing.

[9] We focus on the time period of the International Consortium for Atmospheric Research on Transport and Transformation (ICARTT) 2004 summer (July through August 2004) campaign. Satellite and model data is binned into four $4^\circ \times 4^\circ$ boxes along the direction of prevailing winds downwind of the highly populated U.S. northeastern seaboard. By breaking up the region into boxes we aim to analyze whether the sensitivity of clouds to pollution changes with age because of wet scavenging or gas-to-particle conversion. Aircraft measurements of cloud properties and trace gases from the National Oceanic and Atmospheric Administration (NOAA) WP-3D research aircraft during ICARTT permitted similar comparisons in situ.

2. Methods

2.1. Satellite Retrievals

[10] Terra and Aqua MODIS Collection 4 Level 2 retrievals are used to provide pixel-level cloud-top temperature and pressure, cloud-top effective radius (r_e), cloud optical thickness (τ_c), cloud liquid water path (*LWP*) from their respective morning and afternoon overpasses. For low-level clouds, cloud-top temperatures and pressures are determined using the infrared window 11-μm band temperature at 5 km spatial resolution [*Platnick et al.*, 2003]. Retrievals of r_e and τ_c are made using simultaneous measurements in six visible and near-infrared bands at 1 km spatial resolution. MODIS r_e (τ_c) may be biased toward larger (smaller) sizes in broken cloud fields because of subpixel cloudiness [*Platnick et al.*, 2003] and three-dimensional cloud structure [*Marshak et al.*, 2006]. However, applications of the technique to retrieval of r_e and τ_c in stratiform cloud compare well with in situ measurements [e.g., *Platnick et al.*, 2001]. Also, in this study we focus on difference and trends, in which the effect of bias errors should be minimized.

[11] We apply a correction factor of 8/9 to the Collection 4 MODIS *LWP*, because it is incorrectly computed using the formula $LWP = 3/4\tau_c r_e$, and should instead be $LWP = 2/3\tau_c r_e$.

2.2. Tracer Transport Model Output

[12] The Lagrangian particle dispersion model FLEXPART [*Stohl et al.*, 2005] uses European Centre for Medium-Range Weather Forecasts (ECMWF) meteorological analyses to advect passive particulate and gaseous tracers. It contains source functions and meteorology, but no representation of chemical reactions or deposition. For the ICARTT period over the western North Atlantic, FLEXPART is driven by the ECMWF analyses at 60 vertical model levels, with a horizontal resolution of 0.36° nested within a 1° resolution global domain. We consider here only the advection of ''regional'' tracers from North American anthropogenic emission sources as described by the 1999 Environmental Protection Agency (EPA) National Emission Inventory (NEI). The NEI has a resolution of 4 km [*Frost et al.*, 2006], but larger point sources (e.g., power plants) are treated as points. Tracer fields were stored in output files with a resolution of $1/4^\circ \times 1/3^\circ$ and 23 layers every 2 hours. FLEXPART has been validated with measurement data from large-scale tracer experiments [*Stohl et al.*, 1998] and has been employed previously to examine the transport of pollution [e.g., *Stohl and Trickl*, 1999] and forest fire emissions [*Spichtinger et al.*, 2001; *Forster et al.*, 2001]. *Warneke et al.* [2006] made comparisons between ship- and air-based measures of CO and FLEXPART predictions. FLEXPART yielded passive anthropogenic CO concentrations in the marine surface layer that were about 50% higher

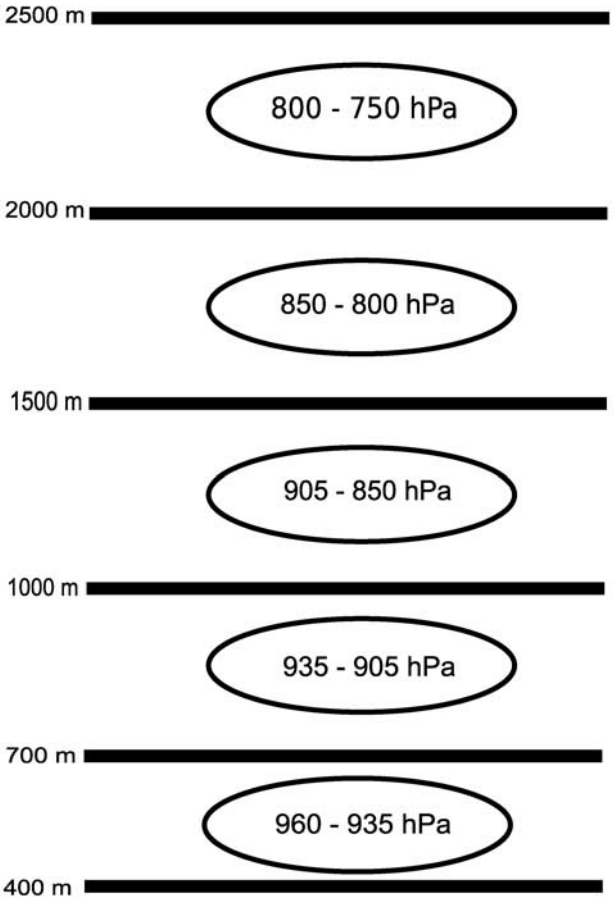

Figure 2. Vertical colocation of satellite and chemical transport model data used in this study. Ovals indicate the range of MODIS cloud-top pressures that fall between the FLEXPART model level heights (solid lines).

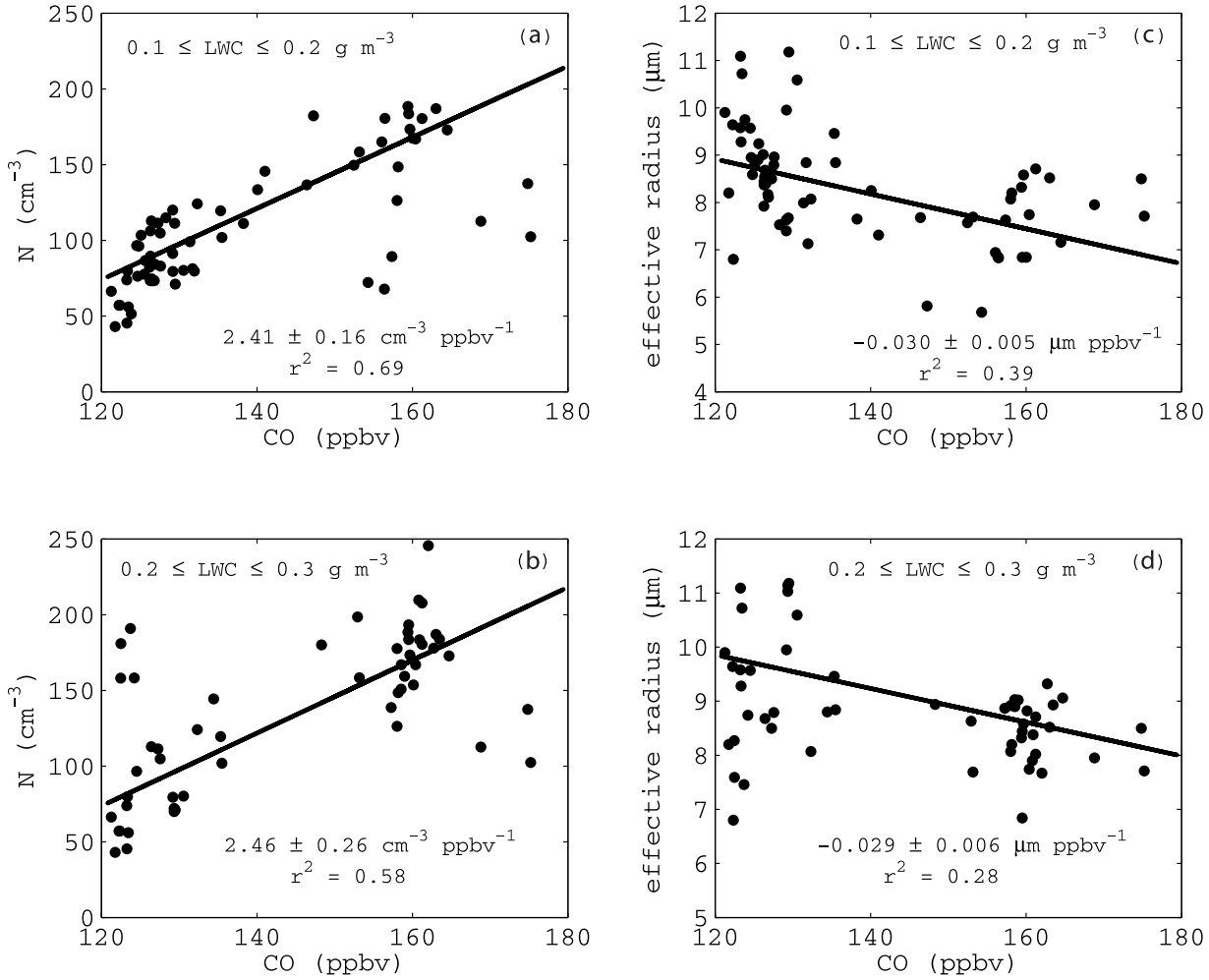

Figure 3. (a and b) *N*-CO and (c and d) r_e-CO relationships from aircraft measurements of low-level clouds within analysis box 1. Dots represent 10-s averages in CO, *N*, and r_e. The solid line provides a linear fit to the data. Data are binned for *LWC* values between 0.1 and 0.2 g m^{-3} (Figures 3a and 3c) and 0.2 and 0.3 g m^{-3} (Figures 3b and 3d).

than those actually measured. The difference dropped to approximately 20% at heights between 0.5 and 2.5 km, and close to zero at higher altitudes.

2.3. Aircraft Data

[13] For ICARTT, the Particle Measurement Systems (PMS) Forward Scattering Spectrometer Probe (FSSP-100) [*Dye and Baumgardner*, 1984] and NOAA's PMS OAP-2DC [*Heymsfield and Parrish*, 1978] was integrated onto the WP-3D aircraft. Distributions of droplets between 2- and 1500-μm diameter were obtained, from which *N*, liquid water content (*LWC*), and r_e were derived. The FSSP-100 was calibrated with glass beads of known sizes on a regular basis throughout the field project and both instruments were overhauled by Droplet Measurement Technologies (DMT) prior to ICARTT. Mixing ratios of CO were measured using a vacuum ultraviolet (VUV) fluorescence instrument [*Holloway et al.*, 2000]. Instrument background and sensitivity were determined on a periodic basis. For the ICARTT campaign, the instrument had a 1 s detection limit of <1 ppbv, with an estimated accuracy of 2.5%.

2.4. Analysis Technique

[14] Midlatitude cyclones are the principal pathway for the transport of pollution from the U.S. eastern seaboard to the western North Atlantic [*Merrill and Moody*, 1996; *Moody et al.*, 1996]. Four 4° × 4° analysis boxes are prescribed to align along this pathway, while avoiding emission sources outside the U.S. eastern seaboard (e.g., Halifax, Nova Scotia) (Figure 1).

[15] For MODIS cloud-top temperatures greater than 0°C, FLEXPART output is colocated temporally with MODIS overpass times, and vertically with MODIS derived cloud-top pressures. For example, a 1520 UTC satellite granule is matched up temporally with the 1400–1600 UTC FLEXPART output field. The scheme for vertical colocation is illustrated in Figure 2: Satellite cloud-top pressures ranging between 905 to 850 hPa are colocated with the average from the FLEXPART concentrations at 1 km and 1.5 km level. MODIS low-level cloud properties are then gridded with the FLEXPART CO concentration field into 0.5 × 0.5 cells, and then collected into four 4 × 4 analysis boxes (Figure 1).

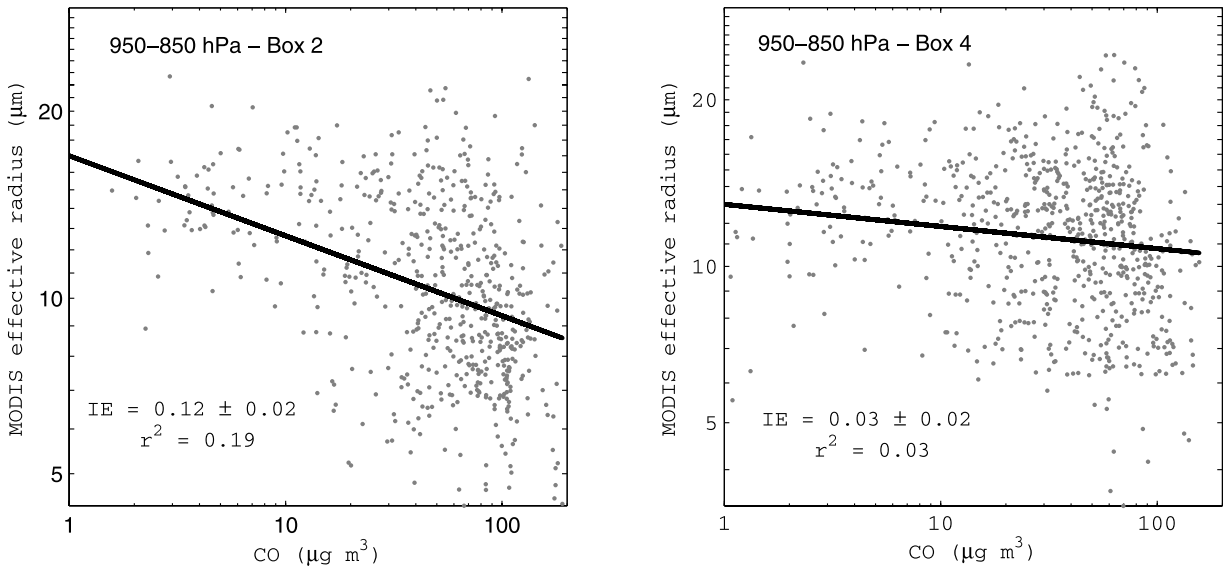

Figure 4. Illustration of how the parameter *IE* (equation (1)) is calculated, shown here for data within boxes 2 and 4 (Figure 1) at levels between 950 and 850 hPa. The lines represent least-squares fits for the slope d ln r_e/d ln CO.

While MODIS and FLEXPART resolutions are both finer than 0.5 × 0.5, a coarser grid is chosen to compensate for two possible sources of error in the placement of FLEXPART fields. These are proportional to (1) strong spatial gradients in pollutant concentrations close to source regions and (2) advection errors. Because both errors are controlled by mixing and are somewhat compensating (as distance downwind increases, gradient errors decrease while advection errors increase) we estimate a general location error of about 10% or 0.5°, assuming that by about 500 km from source regions advection errors dominate and gradient errors are small.

3. Observations

3.1. Pollution-Cloud Relationships in in Situ Data

[16] To examine the relationship between carbon monoxide concentrations and cloud properties, we first look at aircraft measurements. In situ comparisons from within box 1 (Figure 1) are illustrated in Figure 3 (no low-level cloud measurements were made in either boxes 2 through 4 during ICARTT). The data examined are from flights on 9 July and 21 July. The data set is limited, unfortunately, because the WP-3D tended to avoid clouds in the interest of preserving the performance of some of the chemistry probes aboard the plane. To constrain a thermodynamically expected sensitivity of r_e to *LWC*, we binned data into two *LWC* subsets lying between 0.1 and 0.2 g m^{-3} (Figures 3a and 3c) and between 0.2 and 0.3 g m^{-3} (Figures 3b and 3d). The slopes and associated errors are derived from linear least square fits to the data. N ranges between 50 cm^{-3} and 250 cm^{-3}, and higher droplet concentrations are generally associated with greater CO mixing ratios. The fitted slopes are 2.41 ± 0.26 cm^{-3} ppbv^{-1} and 2.46 ± 0.26 cm^{-3} ppbv^{-1} for the 0.1 and 0.2 g m^{-3} (r^2 = 0.69) and 0.2 and 0.3 g m^{-3} (r^2 = 0.58) *LWC* bins, respectively.

[17] Assuming the background concentration for CO is approximately 100 ppbv [*Garrett et al.*, 2006], the fit to the data in Figures 3a and 3b suggests a background cloud droplet concentration of about 30 cm^{-3}. In this case dlnΔN/dlnΔCO is approximately 1, where ΔCO and ΔN are perturbations from the background. Thus the observed correspondence between the perturbations in in situ measurements of N and CO suggests that it is reasonable to use modeled regional CO as a proxy for anthropogenic CCN.

[18] In reality, a perfect correlation between measurements of N and CO should not be expected. This is because CO is slowly oxidized, CCN are scavenged by precipitation, and the supersaturation in and between clouds is variable. Nonetheless, in fresh urban plumes, *Longley et al.* [2005] showed generally high correlation between concentrations of aerosol with sizes between 95 and 470 nm, and CO concentrations. On average, the slope found was 6.0 ± 1.8 cm^{-3} ppbv^{-1}, which is higher than the slope shown in Figure 3. That *Longley et al.* [2005] did not directly examine CCN concentrations may account for some of the difference.

[19] Figures 3c and 3d show that r_e decreases with increasing levels of CO. The fitted slope us −0.030 ± 0.006 μm ppbv^{-1} for the 0.1 and 0.2 g m^{-3} *LWC* bin (r^2 = 0.39) and −0.029 ± 0.006 μm ppbv^{-1} for the 0.2 and 0.3 g m^{-31} *LWC* bin (r^2 = 0.28). While the correlation is weak, it reflects the difficulty of quantifying sensitivities in small data sets of a highly variable system.

3.2. Pollution-Cloud Relationships in FLEXPART and MODIS Data

[20] During the ICARTT period, 72 Terra and Aqua satellite overpasses were matched with FLEXPART output. Within the four analysis boxes, 6074 0.5° × 0.5° cells contained at least 1 pixel with a retrieved cloud-top temperature greater than 0°C. Results were separated into two different ranges of cloud-top pressure, at 950–850 hPa and 850–750 hPa, in order to constrain the weak thermodynamic dependence of cloud r_e on atmospheric temperature [e.g., *Brenguier and Chaumat*, 2001].

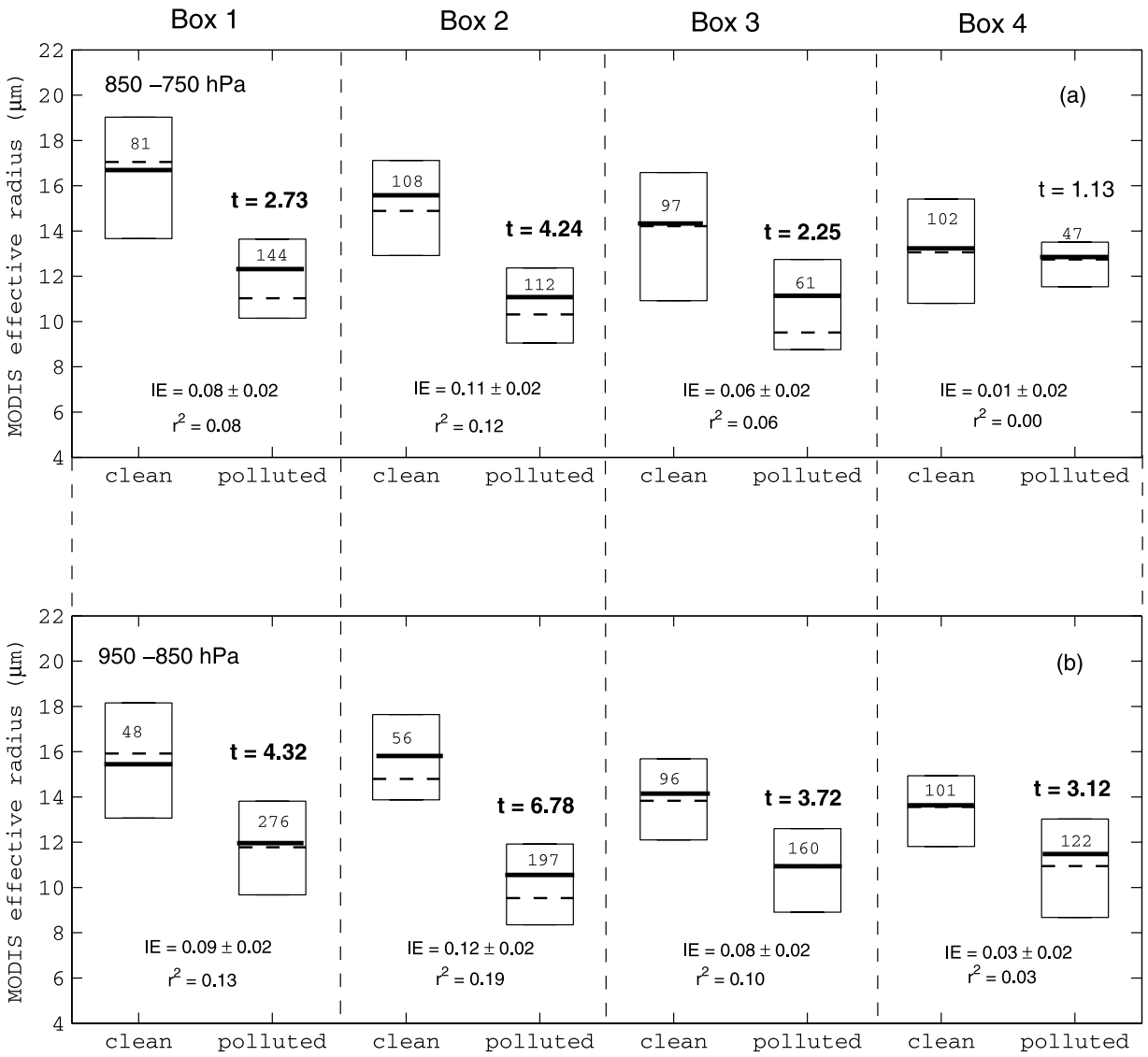

Figure 5. Quartile plots showing comparisons of cloud droplet effective radii under clean (CO $\leq$ 4.6 μg m^{-3}) and polluted (CO $\geq$ 68.8 μg m^{-3}) conditions for (a) cloud-top pressures between 850 and 750 hPa and (b) cloud-top pressures between 950 and 850 hPa, within the four boxes shown in Figure 1. One-sided Student *t*-test values for comparison of the means are shown on top of each polluted box. Bold text indicates the difference in the means is statistically significant at the 95% confidence level. The solid line within each box indicates the mean, and the dashed line indicates the median. The sample size is shown within each box. Values of the indirect effect parameter *IE* for all data in each box, its uncertainty, and the correlation coefficient are shown beneath the quartile bars.

[21] Figures 4 and 5 show the relationship between FLEXPART regional CO and MODIS low-level cloud r_e over the western North Atlantic. We present the data in two ways. First, we employ the indirect effect parameter *IE*, which quantifies the relative change in r_e compared to the relative change in some pollution quantity [*Feingold*, 2003]. In the analysis here,

$$IE = -\frac{d \ln r_e}{d \ln \mathrm{CO}} \tag{1}$$

An example is shown in Figure 4, and the statistics for *IE* in each box are shown in Figure 5. In general, the value of *IE* decreases with distance from the northeastern seaboard to near zero in box 4. The maximum values, of approximately 0.12, are found in box 2 at both levels. The correlation between ln r_e and lnCO was found to be uniformly very low, indicating that factors unrelated to anthropogenic pollution are more important for determining the value of r_e.

[22] Given that there is an absence of strong correlation between ln r_e and lnCO, also shown in Figure 5 are comparisons between r_e distributions in the lower 10th (clean)

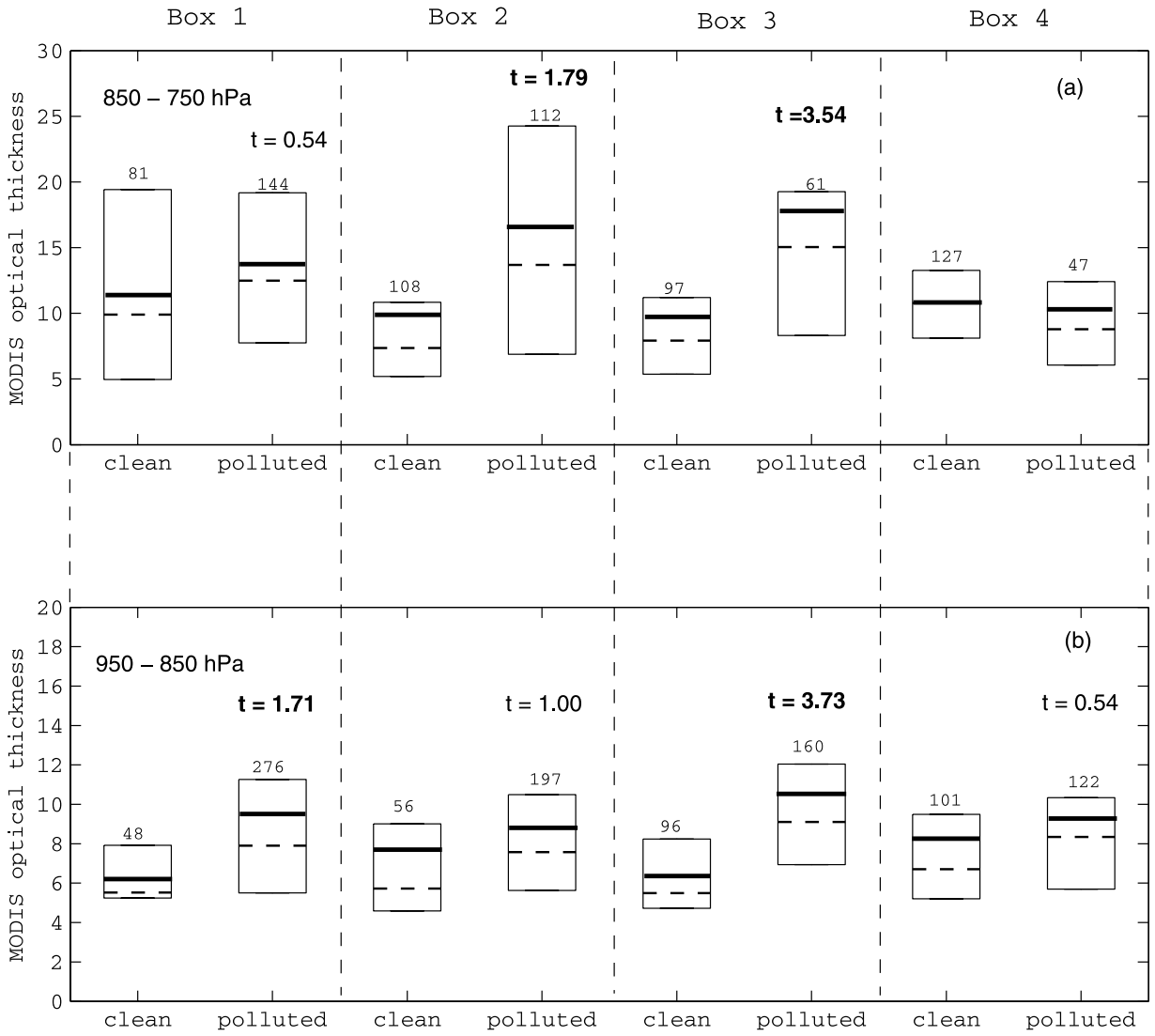

Figure 6. As for Figure 5 except for MODIS retrievals of optical thickness. No one-sided *t*-statistic is given for cases where the mean optical thickness is lower under polluted conditions, in opposition to the first indirect effect hypothesis.

percentile and the upper (polluted) quartile in the FLEXPART regional CO concentration data set, corresponding to threshold values of <4.6 μg m^{-3}and >68.8 μg m^{-3}, respectively. Comparison of these two cohorts in each box enables a more robust measure of whether pollution was affecting cloud properties.

[23] At the 95% confidence level (t >1.6), a one-sided Student t-test confirms the hypothesis that mean r_e is smaller under polluted conditions. The hypothesis holds in every box, except box 4 for cloud-top pressures between 850 and 750 hPa (t = 1.1). The true significance of the differences may be higher than that derived as some portion of the observed variability is due to uncertainties in the spatial matching of satellite and tracer transport model plumes.

[24] We interpret from these results that cloud r_e is affected by pollution downwind of the U.S. northeastern seaboard, but that the sensitivity decreases with distance. The four 4° × 4° boxes cover a horizontal distance of approximately of 1360 km. A likely explanation for the diminished sensitivity is that CCN are scavenged by precipitation, whereas CO is not. Thus, as CCN are rained out, so does the potential for plumes of CO to correspond to smaller cloud r_e [*Garrett et al.*, 2006]. Back trajectory calculations using the HYSPLIT tool (obtained from http://www.arl.noaa.gov/ready/hysplit4.html) indicate an approximate transport time from the northeastern seaboard to box 4, and hence the timescale for CCN removal, of 4 ± 1 days. We emphasize that it would not have been possible to ascertain any evidence of wet scavenging had we used a cloud-dependent soluble species, such as aerosol, as an indicator for pollution.

[25] Plausibly, *IE* might also be affected by gas-to-particle conversion. Primary pollutant trace gases such as sulfur dioxide (SO_2) become oxidized in the atmosphere, and converted to particulate sulfate mass, adding to aerosol droplet nucleation efficiency. Note, for example, that the sensitivity of cloud r_e to pollution plumes is slightly greater

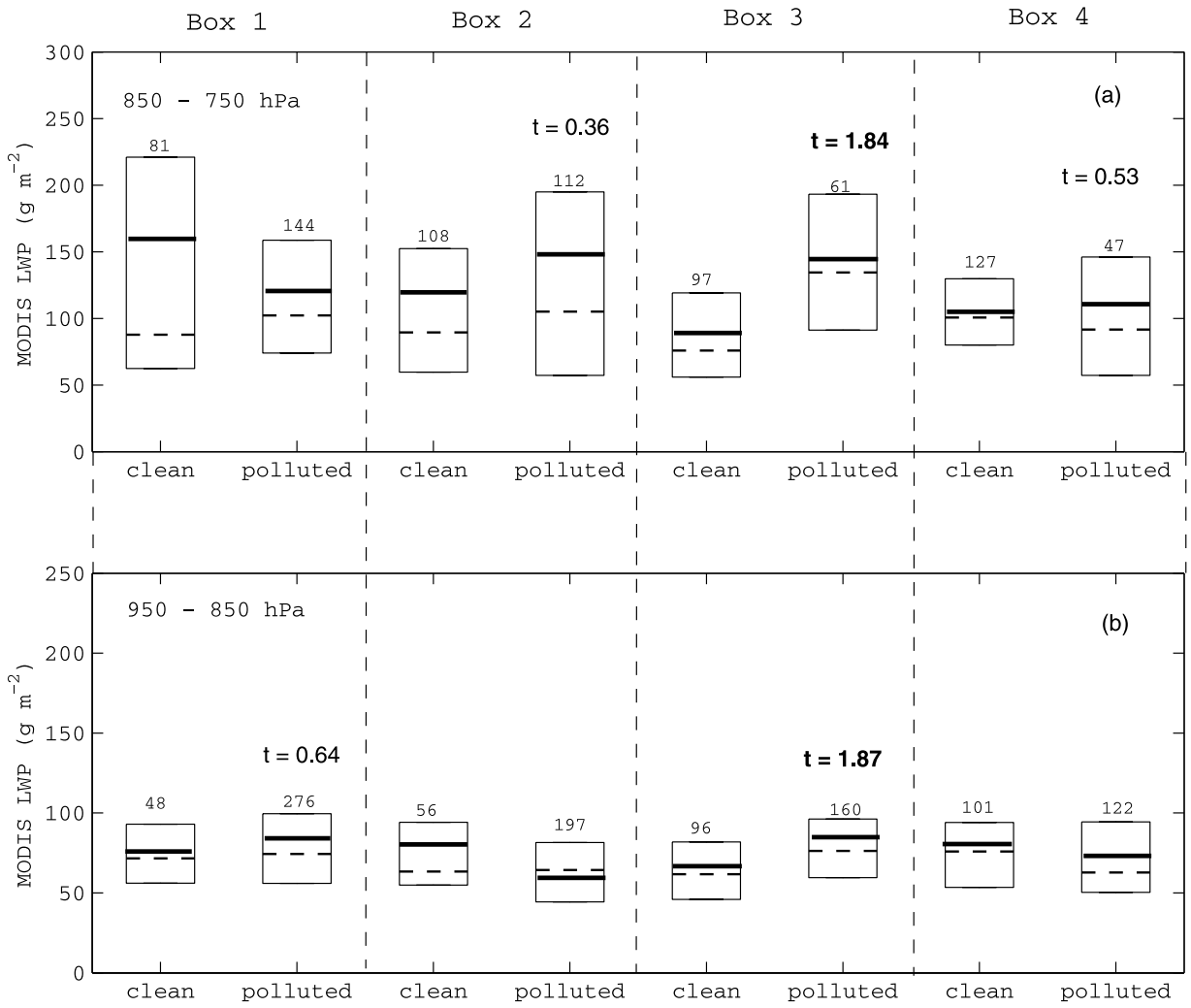

Figure 7. As for Figure 5 except for MODIS liquid water path *LWP* (g m^{-3}). No one-sided *t*-statistic is given for cases where the mean *LWP* is lower under polluted conditions, in opposition to the second indirect effect hypothesis.

in box 2 than in box 1. However, aircraft data obtained within box 1 (for the times shown in Figure 3) showed no evidence of elevated SO_2 concentrations, and no correlation between SO_2 concentrations and cloud properties. Apparently, whatever gas-to-particle conversion of sulfur species that occurred was largely completed before pollution plumes reached box 1, and it did not contribute further to plume evolution (Figure 1).

[26] While there is clear evidence for a first indirect effect in the effective radius retrievals, the signature is less clear in MODIS retrievals of cloud optical thickness τ_c (Figure 6). Only one half of the boxes at both pressure levels showed a statistically significant increase in mean τ_c, although, for these cases, the average magnitude of the increase was 65% under nominally polluted conditions. In box 4, furthest from the northeastern seaboard, neither the 950 to 850 hPa, nor the 850 to 950 hPa levels showed any clear change in τ_c.

[27] Any evidence for a second indirect effect should be expected to show up as an increase in retrievals of cloud *LWP*. The relationship between MODIS *LWP* and FLEXPART regional CO plumes is shown in Figure 7. Only in box 3 was the mean *LWP* significantly higher, by on average 37%. However, because no other boxes showed evidence for this effect, it is difficult to argue for conclusive evidence of a second indirect effect in any of the data.

4. Conclusions

[28] This study has shown how passive fields from a tracer transport model of an insoluble species (in this case carbon monoxide (CO)) can be colocated with cloud fields viewed from satellites, to evaluate effects of anthropogenic aerosol on cloud radiative properties. The technique avoids ambiguities associated with previous studies where aerosol and cloud properties from differing locations and heights had been paired. In addition, we have used here an insoluble pollution tracer rather than, for example, aerosol optical depth. By using this approach, it is possible to quantify pollution concentrations as a parameter genuinely orthogonal to cloud properties.

[29] The study focused on the ICARTT campaign, between 1 July and 15 August 2004. Tracer model pollutant fields were studied downwind of the U.S. northeastern seaboard over the western North Atlantic. High levels of CO were found to be associated with smaller values of cloud droplet effective radius r_e in low-level clouds, at two atmospheric pressure levels below 750 hPa. The indirect effect parameter $IE = -d \ln r_e / d \ln \mathrm{CO}$ was a maximum of 0.12 within a $4^\circ \times 4^\circ$ box about 700 km downwind, but decreased to close to zero approximately 1400 km downwind. This is probably due to wet scavenging of CCN. The inferred CCN lifetime of 4 ± 1 days agrees well with earlier airborne estimates [*Twomey and Wojciechowski*, 1969].

[30] Using a different spaceborne technique, *Bréon et al.* [2002] estimated that the average value of *IE* over oceans globally is 0.085. *Bréon et al.* [2002] calculated *IE* with respect to aerosol optical depth. Because we calculate *IE* with respect to the insoluble tracer CO, our results are not directly comparable. Nonetheless, at least close to pollution sources, we found values of *IE* that were similar. Farther from shore, however, we found the magnitude of *IE* with respect to CO was much smaller than 0.085. We might infer from this comparison that while the sensitivity of low-level cloud to aerosol may be relatively consistent over oceans, the absolute magnitude of the effect diminishes with distance from source regions. Likely, this is because the anthropogenic aerosol have been removed from the polluted air by rain.

[31] No clear evidence was found for a sensitivity to pollution in mean cloud liquid water path *LWP*. Moreover, we also could not conclusively evaluate whether the observed decrease in r_e corresponded to higher cloud optical thickness τ_c, in part because of high ambient variability in *LWP*. In only half of the $4^\circ \times 4^\circ$ boxes observed was the cloud optical thickness τ_c higher under nominally polluted conditions at the 95% confidence level, although in these cases the average difference was large (65%). No statistically significant increase in τ_c was observed, at both pressure levels examined, within the box that was 1360 km downwind of primary source regions.

[32] Thus we have found conditional support for a hypothesis that low-level cloud downwind of the United States northeastern seaboard responds to pollution aerosol, in a manner consistent with the first indirect effect. However, the magnitude of the associated perturbation appears to disappear within several days advection time over the oceans, mostly likely because of wet scavenging of CCN. Also, we find no clear supporting evidence in the data for the hypothesized second indirect effect. While suggestive, the results should not be considered general. This is because they are representative of only a relatively small spatial sample derived from summer, 2004. We intend to extend comparisons to obtain a more comprehensive analysis of the indirect effects of pollution on cloud radiative properties.

[33] **Acknowledgments.** This work is supported through NOAA grant PID2308014 to T.J.G. under the ICARTT field program. Our appreciation goes to John Holloway for providing CO and SO_2 data from the NOAA WP-3D aircraft and Sandeep Namburi for assistance collecting cloud microphysical data.

References

Albrecht, B. (1989), Aerosols, cloud microphysics, and fractional cloudiness, *Science*, *245*, 1227–1230.

Borys, R. D., D. H. Lowenthal, M. Wetzel, F. Herrera, A. Gonzalez, and J. Harris (1998), Chemical and microphysical properties of marine stratiform cloud in the North Atlantic, *J. Geophys. Res.*, *103*, 22,073–22,086.

Brenguier, J.-L., and L. Chaumat (2001), Droplet spectra broadening in cumulus clouds. Part I: Broadening in adiabatic cores, *J. Atmos. Sci.*, *58*, 628–641.

Bréon, F. M., D. Tanré, and S. Generoso (2002), Aerosol effect on cloud droplet size monitored from satellite, *Science*, *295*, 834–838.

Chameides, W., C. Luo, R. Saylor, D. Streets, Y. Huang, M. Bergin, and F. Giorgi (2002), Correlation between model-calculated anthropogenic aerosols and satellite-derived cloud optical depths: Indication of indirect effect?, *J. Geophys. Res.*, *107*(D10), 4085, doi:10.1029/2000JD000208.

Dye, J., and D. Baumgardner (1984), Evaluation of the forward scattering spectrometer probe: I. Electronic and optical studies, *J. Atmos. Oceanic Technol.*, *1*, 329–344.

Feingold, G. (2003), Modeling of the first indirect effect: Analysis of measurement requirements, *Geophys. Res. Lett.*, *30*(19), 1997, doi:10.1029/2003GL017967.

Forster, C., et al. (2001), Transport of boreal forest fire emissions from Canada to Europe, *J. Geophys. Res.*, *106*, 22,887–22,906.

Frost, G. J., et al. (2006), Effects of changing powerplant NO_x emissions on ozone in the eastern United States: Proof of concept, *J. Geophys. Res.*, *111*, D12306, doi:10.1029/2005JD006354.

Garrett, T. J., and P. V. Hobbs (1995), Long-range transport of continental aerosols over the Atlantic Ocean and their effects on cloud structures, *J. Atmos. Sci.*, *52*, 2977–2984.

Garrett, T. J., L. Avey, P. I. Palmer, A. Stohl, J. A. Neuman, C. A. Brock, T. B. Ryerson, and J. S. Holloway (2006), Quantifying wet scavenging processes in aircraft observations of nitric acid and cloud condensation nuclei, *J. Geophys. Res.*, *111*, D23S51, doi:10.1029/2006JD007416.

Hegg, D. A., P. V. Hobbs, and L. F. Radke (1980), Observations of the modification of cloud condensation nuclei in wave clouds, *J. Rech. Atmos.*, *14*, 217–222.

Heymsfield, A. J., and J. L. Parrish (1978), A computational technique for increasing the effective sampling volume of the PMS two-dimensional particle size spectrometer, *J. Appl. Meteorol.*, *17*, 1566–1571.

Holloway, J. S., et al. (2000), Airborne intercomparison of vacuum ultraviolet fluorescence and tunable diode laser absorption measurements of tropospheric carbon monoxide, *J. Geophys. Res.*, *105*, 24,251–24,262.

Hoppel, W. A., J. W. Fitzgerald, G. M. Frick, R. E. Larson, and E. J. Mack (1994), A cloud chamber study of the effect that nonprecipitating water clouds have on aerosol size distributions, *Aerosol Sci. Technol.*, *20*, 1–30.

Johnson, D. W., et al. (2000), An overview of the Lagrangian experiments undertaken during the North Atlantic regional Aerosol Characterisation Experiment (ACE-2), *Tellus, Ser. B*, *52*, 290–320.

Jones, A., D. L. Roberts, and A. Slingo (1994), A climate model study of indirect radiative forcing by anthropogenic sulphate aerosols, *Nature*, *370*, 450–453.

Kaufman, Y. J., I. Koren, L. A. Remer, D. Rosenfeld, and Y. Rudich (2005), The effect of smoke, dust, and pollution aerosol on shallow cloud development over the Atlantic Ocean, *Proc. Natl. Acad. Sci. U. S. A.*, *102*, 11,207–11,212.

Kawamoto, K., T. Hayasaka, I. Uno, and T. Ohara (2006), A correlative study on the relationship between modeled anthropogenic aerosol concentration and satellite-observed cloud properties over east Asia, *J. Geophys. Res.*, *111*, D19201, doi:10.1029/2005JD006919.

Lohmann, U., and G. Lesins (2002), Stronger constraints on the anthropogenic indirect aerosol effect, *Science*, *298*, 1012–1015.

Longley, I. D., D. W. G. Inglis, M. W. Gallagher, P. I. Williams, J. D. Allan, and H. Coe (2005), Using NO_x and CO monitoring data to indicate fine aerosol number concentrations and emissions factors in three UK conurbations, *Atmos. Environ.*, *39*, 5157–5169.

Marshak, A., S. Platnick, T. Várnai, G. Wen, and R. F. Cahalan (2006), Impact of three-dimensional radiative effects on satellite retrievals of cloud droplet sizes, *J. Geophys. Res.*, *111*, D09207, doi:10.1029/2005JD006686.

Matheson, M. A., J. J. A. Coakley, and W. R. Tahnk (2005), Aerosol and cloud property relationships for summertime stratiform clouds in the northeastern Atlantic from Advanced Very High Resolution Radiometer observations, *J. Geophys. Res.*, *110*, D24204, doi:10.1029/2005JD006165.

Merrill, J. T., and J. L. Moody (1996), Synoptic meteorology and transport during the North Atlantic Regional Experiment (NARE) intensive: Overview, *J. Geophys. Res.*, *101*, 28,903–28,922.

Moody, J. (1996), Meteorological mechanisms for transporting O_3 over the western North Atlantic Ocean: A case study for August 24–29, 1993, *J. Geophys. Res.*, *101*, 29,213–29,228.

Nakajima, T., A. Higurashi, K. Kawamoto, and J. E. Penner (2001), A possible correlation between satellite-derived cloud and aerosol microphysical parameters, *Geophys. Res. Lett.*, *28*, 1171–1174.

Peäjä, T., V.-M. Kerminen, K. Hŷameri, P. Vaattovaara, J. Joutsensaari, W. Junkermann, A. Laaksonen, and M. Kulmala (2005), Effects of SO_2 oxidation on ambient aerosol growth in water and ethanol vapours, *Atmos. Chem. Phys.*, *5*, 767–779.

Platnick, S., and S. Twomey (1994), Determining the susceptibility of cloud albedo to changes in droplet concentration with the Advanced Very High Resolution Radiometer, *J. Appl. Meteorol.*, *33*, 334–347.

Platnick, S., J. Y. Li, M. D. King, H. Gerber, and P. V. Hobbs (2001), A solar reflectance method for retrieving the optical thickness and droplet size of liquid water clouds over snow and ice surfaces, *J. Geophys. Res.*, *106*, 15,185–15,200.

Platnick, S., M. King, S. A. Ackerman, W. Menzel, B. Baum, J. Riedi, and R. Frey (2003), The MODIS cloud products: Algorithms and examples from Terra, *IEEE Trans. Geosci. Remote Sens.*, *41*, 459–473.

Quaas, J., and O. Boucher (2005), Constraining the first aerosol indirect radiative forcing in the LMDZ GCM using POLDER and MODIS satellite data, *Geophys. Res. Lett.*, *32*, L17814, doi:10.1029/2005GL023850.

Quaas, J., O. Boucher, and F.-M. Bréon (2004), Aerosol indirect effects in POLDER satellite data and the Laboratoire de Météorologie Dynamique-Zoom (LMDZ) general circulation model, *J. Geophys. Res.*, *109*, D08205, doi:10.1029/2003JD004317.

Quaas, J., O. Boucher, and U. Lohmann (2006), Constraining the total aerosol indirect effect in the LMDZ and ECHAM4 GCMs using MODIS satellite data, *Atmos. Chem. Phys.*, *6*, 947–955.

Schwartz, S. E., Harshvardham, and C. M. Benkovitz (2002), Influence of anthropogenic aerosol on cloud optical depth and albedo shown by satellite measurements and chemical transport modeling, *Proc. Natl. Acad. Sci. U. S. A.*, *99*, 1784–1789.

Sekiguchi, M., T. Nakajima, K. Suzuki, K. Kawamoto, A. Higurashi, D. Rosenfeld, I. Sano, and S. Mukai (2003), A study of the direct and indirect effects of aerosols using global satellite data sets of aerosol and cloud parameters, *J. Geophys. Res.*, *108*(D22), 4699, doi:10.1029/2002JD003359.

Spichtinger, N., M. Wenig, P. James, T. Wagner, U. Platt, and A. Stohl (2001), Satellite detection of a continental-scale plume of nitrogen oxides from boreal forest fires, *Geophys. Res. Lett.*, *28*, 4579–4582.

Stohl, A. (2001), A one-year Lagrangian "climatology" of airstreams in the Northern Hemisphere troposphere and lowermost stratosphere, *J. Geophys. Res.*, *106*, 7263–7279.

Stohl, A., and T. Trickl (1999), A textbook example of long-range transport: Simultaneous observation of ozone maxima of stratospheric and North American origin in the free troposphere over Europe, *J. Geophys. Res.*, *104*, 30,445–30,462.

Stohl, A., M. Hittenberger, and G. Wotawa (1998), Validation of the Lagrangian particle dispersion model FLEXPART against large-scale tracer experiment data, *Atmos. Environ.*, *32*, 4245–4264.

Stohl, A., C. Forster, A. Frank, P. Seibert, and G. Wotawa (2005), Technical note: The Lagrangian particle dispersion model FLEXPART version 6.2, *Atmos. Chem. Phys.*, *5*, 2461–2474.

Twomey, S. (1977), The influence of pollution on the shortwave albedo of clouds, *J. Atmos. Sci.*, *34*, 1149–1152.

Twomey, S., and T. A. Wojciechowski (1969), Observations of the geographical variation of cloud nuclei, *J. Atmos. Sci.*, *26*, 684–688.

Warneke, C., et al. (2006), Biomass burning and anthropogenic sources of CO over New England in the summer 2004, *J. Geophys. Res.*, *111*, D23S15, doi:10.1029/2005JD006878.

L. Avey and T. J. Garrett, Meteorology Department, University of Utah, 135 S 1460 E, Room 819, Salt Lake City, UT 84112-0110, USA. (tgarrett@met.utah.edu)

A. Stohl, Norwegian Institute for Air Research, N-2027 Kjeller, Norway.